

## S1 Some Photographs before and after the ecological restoration program

Before ecological restoration program



After ecological restoration program



Figure S1 Some photographs before and after the ecological restoration program in the study area.

## S2 Computation of the SPEI

The computation of the SPEI is as follows:

Drought indices used in the study are constructed based on precipitation and potential evapotranspiration(Vicente-Serrano et al., 2010).

Firstly, Potential evapotranspiration (PET) is calculated by Thornthwaite method in equation 1:

$$PET=16K\left(\frac{10T}{I}\right)^m \quad (1)$$

Where  $T$  is the monthly mean temperature ( $^{\circ}\text{C}$ );  $I$  is a heat index, which is calculated as the sum of 12 monthly index values;  $m$  is a coefficient depending on  $I$ ;  $m = 6.75 \times 10^{-7} I^3 - 7.71 \times 10^{-5} I^2 + 1.79 \times 10^{-2} I + 0.492$ ; and  $K$  is a correction coefficient computed as a function of the latitude and month.

Secondly, the SPEI is based on a climatic water balance which is determined by the difference between precipitation ( $P$ ) and potential evapotranspiration (PET) for the month  $i$ :

$$D_i = P_i - PET_i \quad (2)$$

The calculated  $D_i$  values are aggregated at different time scales, following the same procedure as that for the SPI. The difference  $D_{i,j}^k$  in a given month  $j$  and year  $i$  depends on the chosen time scale  $k$ . For example, the accumulated difference for  $l$  month in a particular year  $i$  with a 12-month time scale is calculated using:

$$X_{i,j}^k = \sum_{l=13-k+j}^{12} D_{i-1,l} + \sum_{l=1}^j D_{i,l}, \text{ if } j < k, \text{ and} \\ X_{i,j}^k = \sum_{l=j-k+1}^j D_{i,l}, \text{ if } j \geq k \quad (3)$$

Where  $D_{i,l}$  is the P-PET difference in the first month of year  $i$ . Thirdly, the log-logistic distribution was selected for standardizing the  $D$  series to obtain the SPEI.

The probability density function of log-logistic distributed variable is expressed as:

$$f(x) = \frac{\beta}{a} \left(\frac{x-\gamma}{a}\right)^{\beta-1} \left[1 + \left(\frac{x-\gamma}{a}\right)^{\beta}\right]^{-2} \quad (4)$$

where  $\alpha$ ,  $\beta$ , and  $\gamma$  are scale, shape, and origin parameters respectively. Thus, the probability distribution function of the  $D$  series is given by:

$$f(x) = \left[ 1 + \left( \frac{\alpha}{x - \gamma} \right)^\beta \right] \left[ 1 + \left( \frac{\alpha}{x - \gamma} \right)^\beta \right]^{-1} \quad (5)$$

The SPEI can easily be obtained as the standardized values of  $f(x)$ .

$$SPEI = W - \frac{C_0 + C_1W + C_2W^2}{1 + d_1W + d_2W^2 + d_3W^3} \quad (6)$$

where  $W = \sqrt{-2\ln(P)}$  for  $P \leq 0.5$  and  $P$  is the probability of exceeding a determination  $D$  value,  $P = 1 - f(x)$ . If  $P > 0.5$ , then  $P$  is replaced by  $1 - P$  and the sign of the resultant SPEI is reversed. The constants are  $C_0 = 2.515517$ ,  $C_1 = 0.802853$ ,  $C_2 = 0.010328$ ,  $d_1 = 1.432788$ ,  $d_2 = 0.189269$ , and  $d_3 = 0.001308$ . **The classification of drought based on SPEIs is listed in Table S1**

Table S1. Drought classification of SPEI

	Extreme drought	Severe drought	Moderate drought	Slight drought	Normal
SPEI or SPI	$\leq -2$	$\leq -1.5$	$\leq -1.0$	$\leq -0.5$	0

### S3. Route of three large-scale field investigation surveys

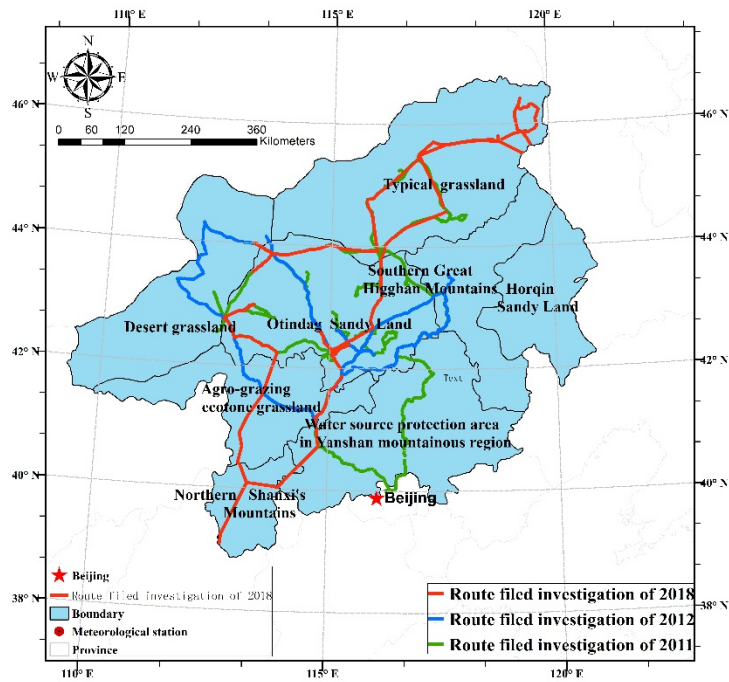


Figure S2 Routes of three large-scale field investigation surveys

#### S4 Brief of Back Propagation (BP) neural network

The BP neural network model has been used in remote sensing image classification (Gao et al., 2018), the parameter inversion of remote sensing (Huang et al., 2018), the pattern recognition (Kumar et al., 2016), and so on. The main principle of BP neural network is as follows:

(1) Forward propagation of operating signal: the input signal is propagated from the input layer, via the hidden layer, to the output layer. During the forward propagation of operating signal, the weight value and offset value of the network are maintained constant and the status of each layer of neuron will only exert an effect on that of the next layer of neuron. In case that the expected output cannot be achieved in the output layer, it can be switched into the back propagation of error signal (Ju et al., 2009).

(2) Back propagation of error signal: the difference between the real output and expected output of the network is defined as the error signal; in the back propagation of error signal, the error signal is propagated from the output end to the input layer in a layer-by-layer manner. During the back propagation of error signal, the weight value of the network is regulated by the error feedback. The continuous modification of weight

value and offset value is applied to make the real output of network closer to the expected one. A typical BP neural network model is a fully connected neural network including an input layer, hidden layer, and output layer (Li et al., 2012).

The structure of the BP neural network model in this study is shown in Figure S1. Firstly, the input layers are the temperature (T), precipitation (P) and SPEI of each pixel and the output layer is NDVI of each pixel during reference period. Then, based on the BP neural network method, NDVI-climate model is established using repeated learning. This model is a regional model for all pixels that vegetation growth is only influenced by climate change. Finally, in the predicting period, the temperature, precipitation and SPEI of each pixel are used as input factors to predict the NDVI at the pixel scale based on NDVI-climate model (Figure S3).

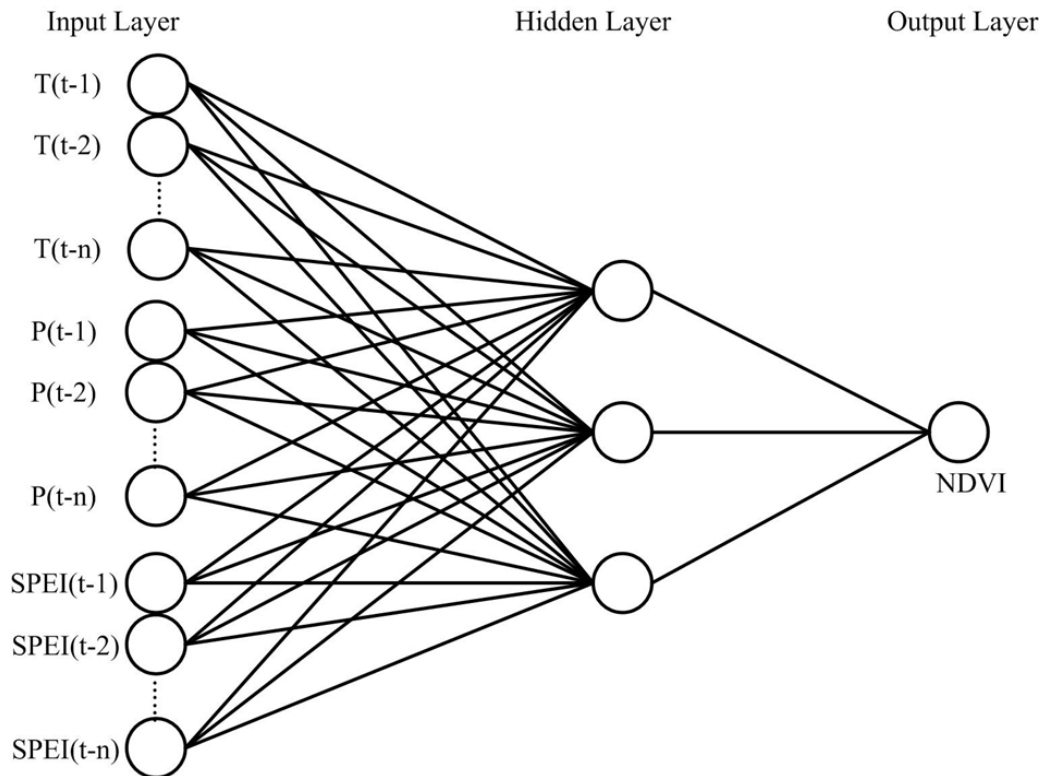


Figure S3 Structure of the BP neural network model of NDVI.

## S5. Identify of drought events and its impacts on NDVI

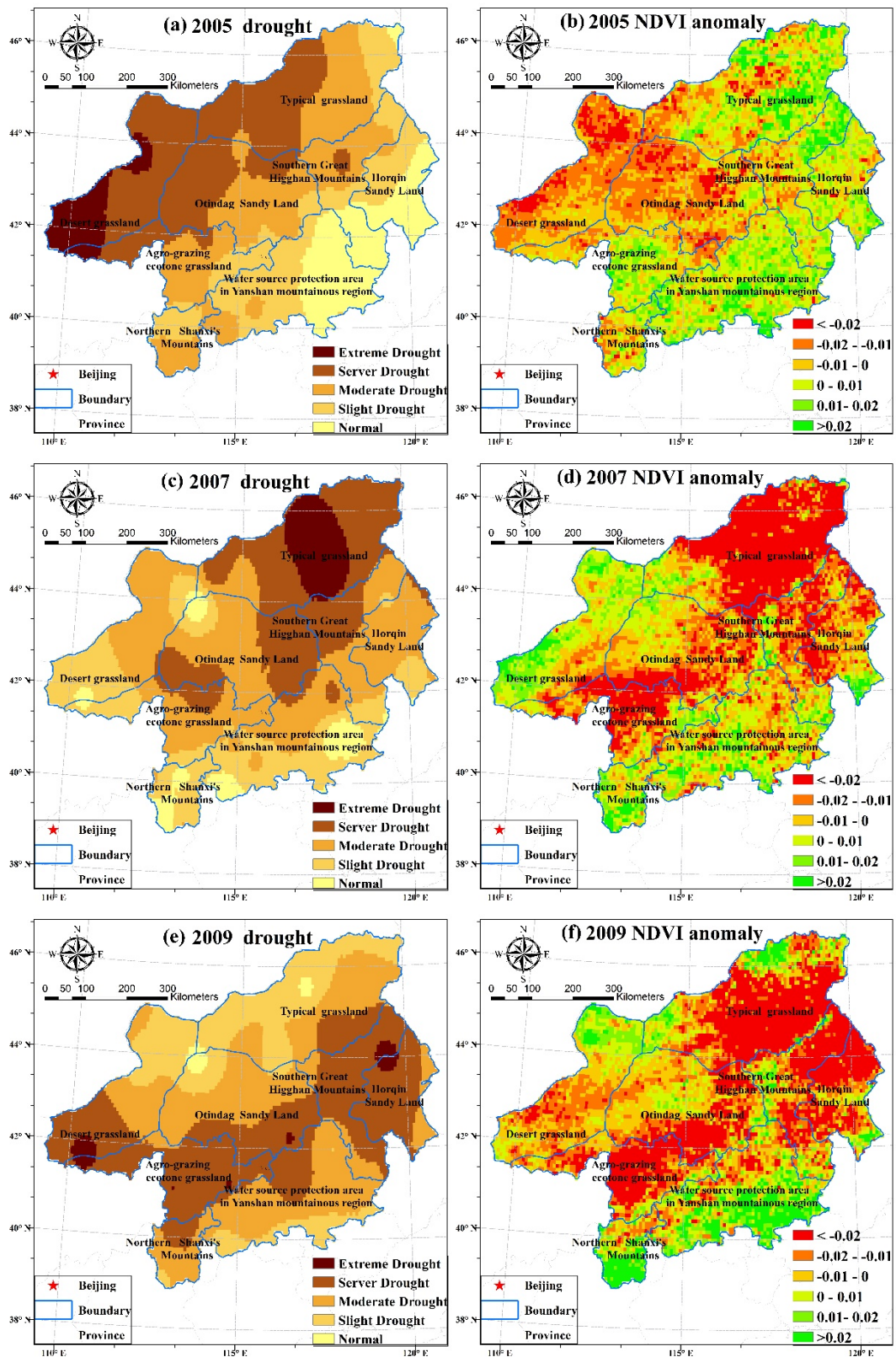


Figure S3 Identify of droughts and its impacts on NDVI change

## S6 Model evaluation of BP network

According to the previous analysis, it can be seen that variations in vegetation

activities have been linked with changes in temperature, precipitation, and SPEI. We assumed that the changes in vegetation were affected mainly by climate change during 1982–1990. Therefore, the neural network model for 1982 to 1990 was established with temperature, precipitation, and SPEI as the input layer and NDVI as the output layer. The total number of samples for the BP neural network model was 65,016, including 45,512 in the training layer, 9,752 in the verification layer, and 9,752 in the test layer. The training and verification results of the BP neural network are shown in Figure S5. The most commonly indicators used for accuracy assessment are the determination coefficient ( $R^2$ ) and the root mean square error (RMSE). The  $R^2$  of the BP neural network was 0.78, and the RMSE was 0.0221. Moreover, the determination coefficient in the training layer, verification layer, and test layer reached more than 0.77. According to the  $R^2$  values, the model simulations correlated well with observed values. To evaluate the reliability of the model further, we analyzed the spatial distribution of observed NDVI and predicted NDVI by BP neural network model in 1991. The spatial distribution of predicted NDVI by the BP neural network model was basically consistent with the observed NDVI. The observed and predicted NDVI showed a decreasing trend from southeast to northwest (Figure S6). The observed NDVI was lower in the Desert grassland and Otindag, and the predicted NDVI by the model was also small in those regions. Therefore, The BP neural network model performed NDVI simulation well.

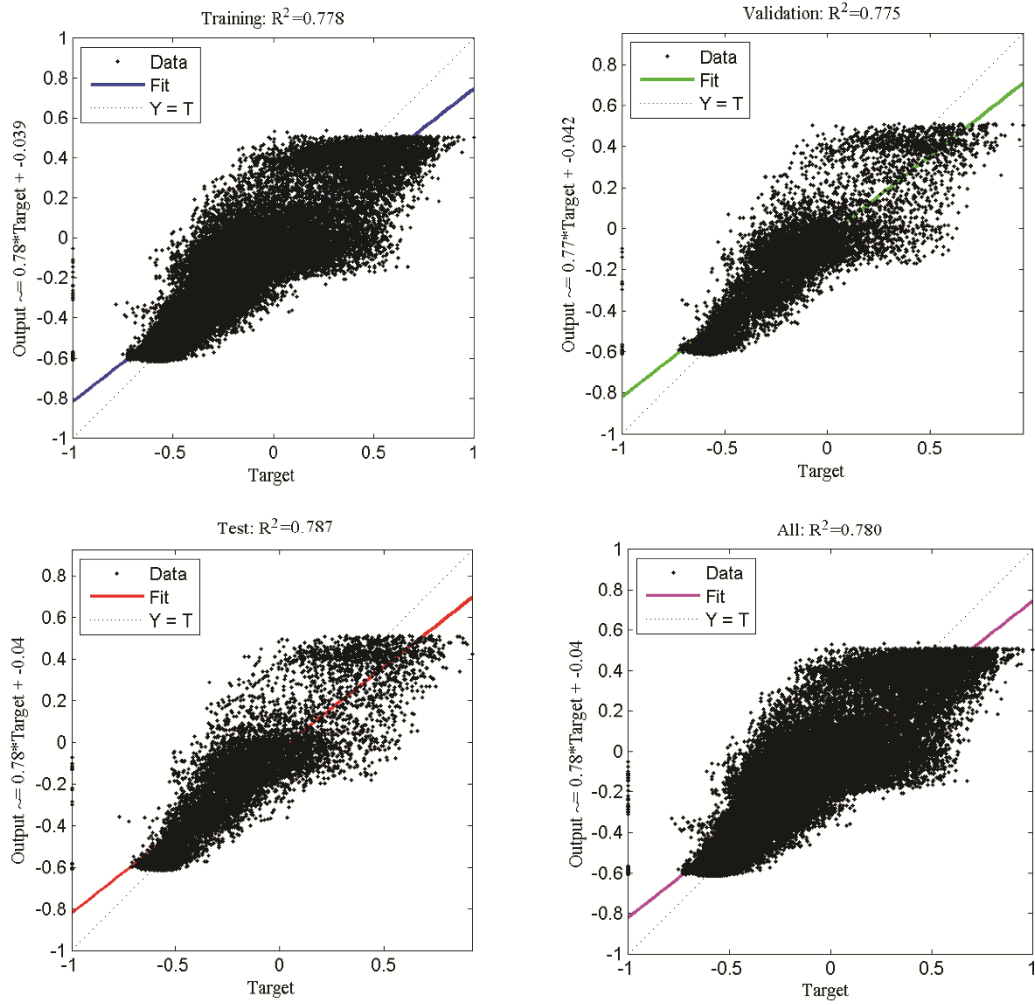


Figure S5. Validation of BP neural network model.

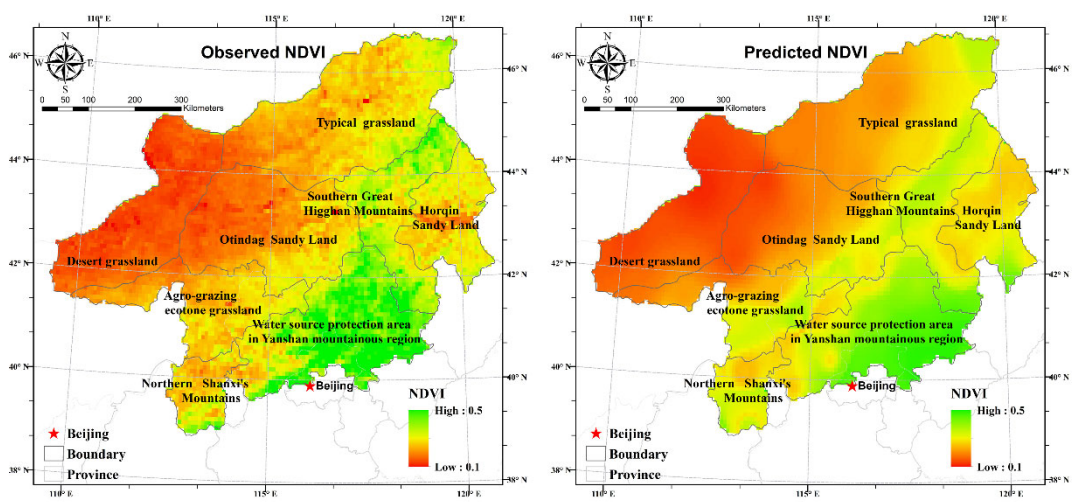


Figure S6. Spatial patterns of observed NDVI and predicted NDVI in 1991.

## Reference

- Gao, Y. N., Li, Q., Wang S. S., & Gao J. F. (2018). Adaptive neural network based on segmented particle swarm optimization for remote-sensing estimations of vegetation biomass. *Remote Sensing of Environment*, **211**, 248–260. <https://doi.org/10.1016/j.rse.2018.04.026>
- Huang, B., Zhao, B., & Song, Y. M. (2018). Urban land-use mapping using a deep convolutional neural network with high spatial resolution multispectral remote sensing imagery. *Remote Sensing of Environment*, **214**, 73–86. <https://doi.org/10.1016/j.rse.2018.04.050>
- Kumar, D. A., Meher, S. K., Kanhar, D., & Kumari, K. P. (2016). Unified granular neural networks for pattern classification. *Neurocomputing*, **216**, 109–125. <https://doi.org/10.1016/j.neucom.2016.07.034>
- Ju, Q., Yu, Z. B., Hao, Z. C., Ou, G. X., Zhao, J., & Liu, D. D. (2009). Division-based rainfall-runoff simulations with BP neural networks and Xinanjiang model. *Neurocomputing*, **72**, 2873–2883. <https://doi.org/10.1016/j.neucom.2008.12.032>
- Li, J., Cheng, J. H., Shi, J. Y., & Huang, F. (2012). Brief Introduction of Back Propagation (BP) Neural Network Algorithm and Its Improvement. *Advances in Computer Science and Information Engineering*, Springer Berlin Heidelberg, 553–558. [https://doi.org/10.1007/978-3-642-30223-7\\_87](https://doi.org/10.1007/978-3-642-30223-7_87)
- Vicente-serrano, S. M., Begueria, S., & Lopez-Moreno, J.I., (2015). A Multiscalar Drought Index Sensitive to Global Warming: The Standardized Precipitation Evapotranspiration Index. *Journal of Climate*, **23**, 1696–1718. <http://doi.org/10.1175/2009JCLI2909.1>.